The EMBO Journal (2008) 27, 1974–1984 | © 2008 European Molecular Biology Organization | All Rights Reserved 0261-4189/08
www.embojournal.org

THE EMBO JOURNAL

Stress-protective signalling of prion protein is corrupted by scrapie prions

Angelika S Rambold[1], Veronika Müller[1], Uri Ron[2], Nir Ben-Tal[2], Konstanze F Winklhofer[1,3] and Jörg Tatzelt[1,3,*]

[1]Department of Biochemistry, Neurobiochemistry, Ludwig-Maximilians-University Munich, München, Germany and [2]Department of Biochemistry, George S Wise Faculty of Life Sciences, Tel Aviv University, Ramat Aviv, Israel

Studies in transgenic mice revealed that neurodegeneration induced by scrapie prion (PrP^{Sc}) propagation is dependent on neuronal expression of the cellular prion protein PrP^{C}. On the other hand, there is evidence that PrP^{C} itself has a stress-protective activity. Here, we show that the toxic activity of PrP^{Sc} and the protective activity of PrP^{C} are interconnected. With a novel co-cultivation assay, we demonstrate that PrP^{Sc} can induce apoptotic signalling in PrP^{C}-expressing cells. However, cells expressing PrP mutants with an impaired stress-protective activity were resistant to PrP^{Sc}-induced toxicity. We also show that the internal hydrophobic domain promotes dimer formation of PrP and that dimerization of PrP is linked to its stress-protective activity. PrP mutants defective in dimer formation did not confer enhanced stress tolerance. Moreover, in chronically scrapie-infected neuroblastoma cells the amount of PrP^{C} dimers inversely correlated with the amount of PrP^{Sc} and the resistance of the cells to various stress conditions. Our results provide new insight into the mechanism of PrP^{C}-mediated neuroprotection and indicate that pathological PrP conformers abuse PrP^{C}-dependent pathways for apoptotic signalling.

The EMBO Journal (2008) **27,** 1974–1984. doi:10.1038/emboj.2008.122; Published online 19 June 2008
Subject Categories: signal transduction; molecular biology of disease
Keywords: apoptosis; dimer; prion; scrapie; stress-protective

Introduction

Prion diseases in humans and other mammals are neurodegenerative diseases characterized by the accumulation of an abnormally folded prion protein, designated PrP^{Sc}, which is the essential constituent of infectious prions. PrP^{Sc} is a self-propagating isoform of the cellular prion protein (PrP^{C}) with distinct biochemical and biophysical properties, such as a high content in β-sheet structures, insolubility in detergent buffers and increased resistance to proteolytic digestion (reveiwed in Weissmann *et al*, 1996; Prusiner *et al*, 1998; Collinge, 2001; Chesebro, 2003; Aguzzi and Polymenidou, 2004). PrP^{C} is essential for the pathogenesis of prion diseases. Mice with a targeted disruption of the PrP gene (PRNP) are resistant to prion diseases and to the propagation of infectious prions (Büeler *et al*, 1993). Moreover, neuronal expression of PrP^{C} seems to be required to mediate neurotoxic effects of scrapie prion propagation. The first indication for such a role of PrP^{C} emerged from elegant grafting experiments (Brandner *et al*, 1996), a finding later supported by a conditional cell-type-specific PrP knockout mouse model (Mallucci *et al*, 2003) and transgenic mice expressing PrPΔGPI, an anchorless PrP mutant (Chesebro *et al*, 2005). Moreover, different mouse models revealed that PrP can acquire a neurotoxic potential in the absence of PrP^{Sc}/prion propagation (reviewed in Winklhofer *et al*, 2008). One class of such toxic PrP mutants is characterized by a deleted internal hydrophobic domain (HD) (Shmerling *et al*, 1998; Baumann *et al*, 2007; Li *et al*, 2007). PrPΔHD is complex glycosylated and linked to the plasma membrane through a glycosylphosphatidylinositol (GPI) anchor (Winklhofer *et al*, 2003b), indicating that this neurotoxic mutant is at the same cellular locale as PrP^{C}. Indeed, results from different mouse models were interpreted in such a way that neurotoxicity of PrPΔHD is linked to a PrP^{C}-dependent signalling pathway (Shmerling *et al*, 1998; Baumann *et al*, 2007; Li *et al*, 2007).

In contrast to the toxic activity of pathological PrP conformers appears to be the physiological function of PrP^{C}. First hints about the activity of PrP^{C} to confer enhanced tolerance to stress emerged from experiments with primary neurons (Kuwahara *et al*, 1999). Using stroke models in rats and mice, it was then demonstrated that PrP^{C} has a neuroprotective activity after an ischaemic insult (McLennan *et al*, 2004; Shyu *et al*, 2005; Spudich *et al*, 2005; Weise *et al*, 2006; Mitteregger *et al*, 2007). These findings in transgenic animals were complemented and corroborated by several studies in cultured cells supporting the idea that PrP^{C} can modulate signalling cascades, in particular stress-protective pathways (Westergard *et al*, 2007).

We now show that stress-protective signalling of PrP^{C} is dependent on the internal HD and the C-terminal GPI anchor. Furthermore, our data provide evidence for a switch from antiapoptotic to pro-apoptotic signalling of PrP^{C} induced by neurotoxic PrP mutations and scrapie prions.

Results

The stress-protective activity of PrP^{C} is dependent on the GPI anchor and the internal HD

From previous studies in transgenic mice and cultured cells, it emerged that expression of PrP^{C} can confer enhanced stress tolerance. As a cell culture system to analyse this activity, we employed transiently transfected SH-SY5Y cells, which are characterized by extremely low levels of endogenous PrP^{C}

*Corresponding author. Department of Biochemistry, Neurobiochemistry, Ludwig-Maximilians-University Munich, Schillerstrasse 44, Munich D-80336, Germany. Tel.: +49 89 2180 74442; Fax: +49 89 2180 75415; E-mail: Joerg.Tatzelt@med.uni-muenchen.de
[3]Senior authors

Received: 29 April 2008; accepted: 30 May 2008; published online: 19 June 2008

(Rambold *et al*, 2006). Cells were exposed to the excitotoxin kainate and apoptotic cell death was determined by the detection of activated caspase-3. Ectopic expression of wild-type (wt) PrP, but not PrPΔN, significantly enhanced survival of cells exposed to kainate (Figure 1B), corroborating results obtained in mice models (Mitteregger *et al*, 2007).

To identify additional domains of PrP^C essential for the stress-protective activity, a variety of PrP mutants were analysed (Figure 1A). It turned out that PrP needs to be attached to the plasma membrane through a GPI anchor: PrP-CD4, which contains a heterologous C-terminal transmembrane domain instead of the GPI anchor (Taraboulos *et al*, 1995; Winklhofer *et al*, 2003b), showed no antiapoptotic activity (Figure 1B). The stress-protective activity was also lost when the short internal HD (amino acids 113–133) was deleted (Figure 1B). Moreover, deletion of the HD induces a switch from antiapoptotic to pro-apoptotic signalling. Apoptotic cell death was significantly increased in cells expressing PrPΔHD (Figure 1B and C). In line with the protective activity of PrP^C against PrPΔHD-induced toxicity in transgenic animals, co-expression of wt PrP alleviated the pro-apoptotic activity of PrPΔHD in SH-SY5Y cells (Figure 1C).

Notably, deletion of the HD or the N terminus seems not to interfere with maturation and cellular trafficking of PrP. Similarly to wt PrP, PrPΔHD and PrPΔN are complex glycosylated and targeted to detergent-insoluble microdomains at the plasma membrane (Figure 1D) (Winklhofer *et al*, 2003b). PrP-CD4 is also complex glycosylated and present at the plasma membrane, but does not localize to detergent-insoluble microdomains (Figure 1D).

The HD mediates dimer formation of PrP^C

After having shown that the HD is required for the stress-protective activity of PrP^C, we sought to analyse the role of the HD in mediating this effect. Signalling by cell surface proteins is often linked to dimer formation, and PrP dimers were reported in previous publications (Priola *et al*, 1995; Meyer *et al*, 2000), with the HD as a putative dimerization domain (Warwicker, 2000).

To examine dimer formation of endogenous PrP^C in N2a cells, we released PrP^C from the plasma membrane through digestion with phosphatidylinositol phospholipase C (PIPLC). The cell culture supernatant was collected and separated by native PAGE. Western blotting revealed two separate bands of endogenous PrP^C (Figure 2A, endogenous PrP^C). Ectopically expressed wt PrP showed a migration pattern similar to that of endogenous PrP^C (Figure 2A, transfected PrP). To provide more evidence that the slower migrating PrP^C species might be a dimer, we replaced serine 131 by cysteine (PrP-S131C). If HD is part of the dimer interface, C131 could form an intermolecular disulphide bond, which would be stable under non-reducing conditions. First, we analysed ectopically expressed wt PrP, PrP-S131C and PrPΔHD by native PAGE. This analysis provided a first clue that the HD is necessary for PrP dimerization; in PrPΔHD-expressing cells only the faster migrating band was detectable, whereas PrP-S131C seemed to stabilize dimer formation (Figure 2B). Next, the supernatants of PIPLC-treated transfected cells were analysed by SDS–PAGE. Under non-reducing conditions, an additional slower migrating band was detectable for PrP-S131C, which disappeared under reducing conditions (Figure 2C). These approaches revealed that (i) endogenous PrP^C can form a dimer, (ii) the HD is part of the dimer interface and (iii) the PrP dimer is present at the plasma membrane. Disulphide-linked dimers of PrP-S131C could also be detected in total cell lysates (Figure 2D) and in detergent-resistant membranes

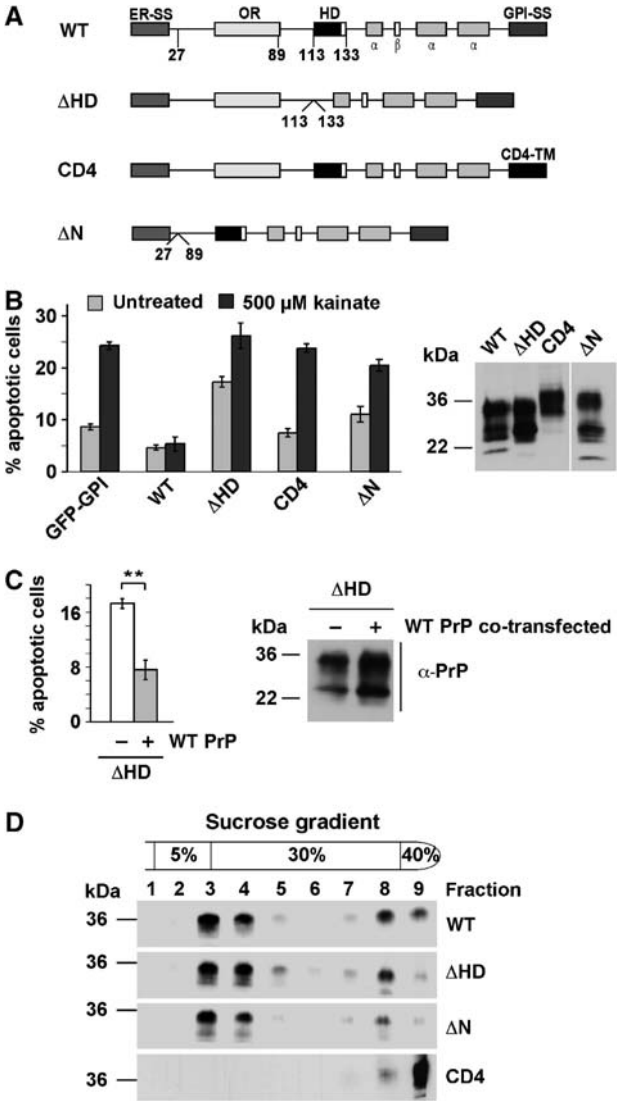

Figure 1 The internal hydrophobic domain and the GPI anchor are necessary for the protective activity of PrP^C. (**A**) Schematic presentation of the PrP mutants analysed. ER-SS: ER signal sequence; OR: octarepeat; HD: hydrophobic domain; α: α-helical region; β: β-strand; GPI-SS: GPI signal sequence; CD4-TM: transmembrane domain of CD4. (**B**) wt PrP^C protects against stress-induced apoptosis. SH-SY5Y cells expressing the constructs indicated were stressed with kainic acid (500 μM) at 37°C for 3 h, fixed, permeabilized, and activation of caspase-3 was analysed by indirect immunofluorescence. In total, 300 transfected cells in at least three independent experiments were counted. The percentage of apoptotic cells among transfected cells is shown. Expression levels were analysed by immunoblotting (right panel). Lane ΔN was positioned to the right side of the gel, all lanes originate from one gel. (**C**) Expression of wt PrP interferes with toxic effects of PrPΔHD. SH-SY5Y cells were transiently transfected with PrPΔHD or PrPΔHD and wt PrP. Apoptotic cell death was determined as described under (B). Expression levels were analysed by immunoblotting (right panel). (**D**) Wt PrP, PrPΔHD, ΔN and CD4 localize to detergent-insoluble microdomains. N2a cells were transiently transfected with the constructs indicated, lysed in ice-cold buffer C and fractionated by a discontinuous sucrose gradient. PrP was detected by immunoblotting using the mAb 3F4. $^{**}P<0.005$.

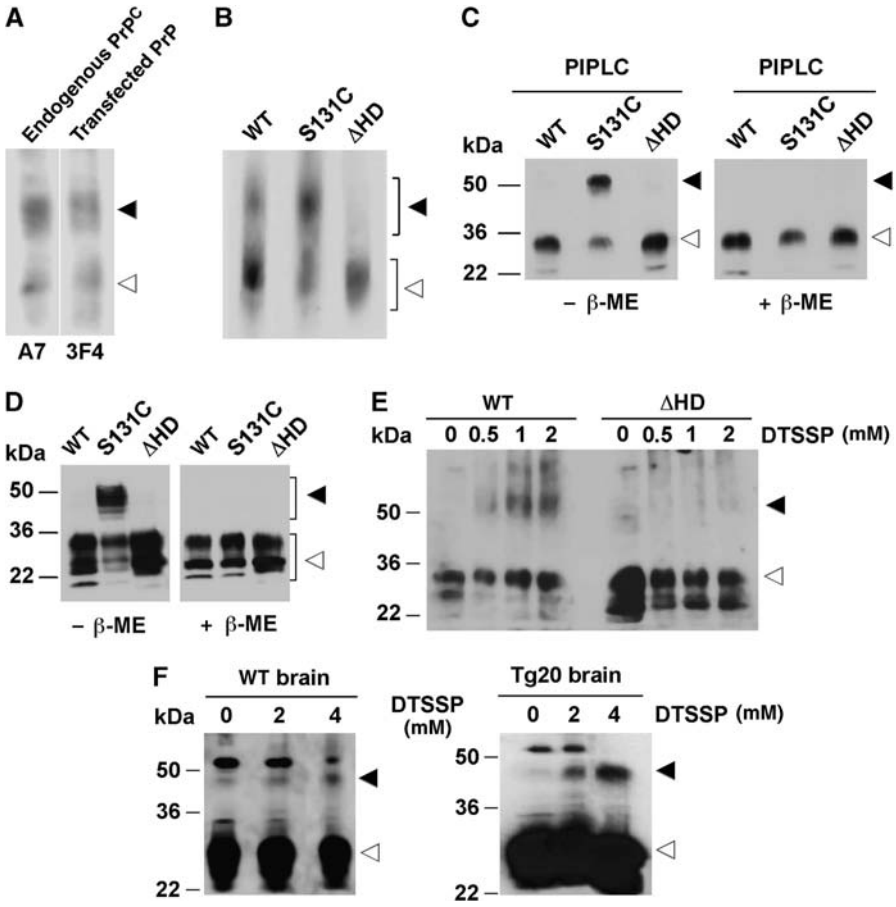

Figure 2 The internal hydrophobic domain promotes homo-dimerization of PrP. (**A**) PrP^C forms dimers. Live N2a cells either untransfected or transiently expressing wt PrP were incubated for 2 h with PIPLC in PBS at 37°C. Proteins present in the cell culture supernatant were analysed by native PAGE using the anti-PrP antiserum A7 (endogenous PrP^C) or the mAb 3F4 (transfected). Western blot membrane was divided for treatment with the specific antibodies indicated, as indicated by a white line. All samples originate form one gel. (**B**–**F**) Dimerization of PrP is dependent on the HD. (B, C) Transiently transfected SH-SY5Y cells were incubated for 2 h with PIPLC in PBS at 37°C and proteins in the cell culture supernatant were analysed by (B) native PAGE or (C) SDS–PAGE under reducing (+β-ME) or non-reducing (−β-ME) conditions. PrP was detected by western blotting using the mAb 3F4. (D) Total cell lysates of transiently transfected SH-SY5Y cells were analysed as described under (C). (E, F) Crude membranes from SH-SY5Y cells, Tg20 or wt mouse brains were incubated for 1 h at 4°C with increasing concentrations of the chemical crosslinker DTSSP. PrP was detected by immunoblotting using the mAb 3F4. Closed arrowheads indicate dimeric forms of PrP, open arrowheads indicate PrP monomers.

(Supplementary Figure 1). As a third approach to analyse dimer formation, we performed crosslinking experiments. Indeed, a PrP crosslink at a size indicative of a PrP dimer was observed for wt PrP in cultured cells and mouse brain, whereas crosslinking of PrPΔHD did not result in such a higher molecular weight species (Figure 2E and F).

To provide further support for the assumption that dimer formation is linked to the stress-protective activity of PrP, we introduced the S131C substitution in those PrP mutants that did not confer enhanced stress tolerance, namely PrPΔHD, PrPΔN and PrP-CD4. Please note that for the construction of ΔHD-S131C the HD deletion was limited to amino acids 112–128. ΔHD-S131C and CD4-S131C showed significantly reduced dimer formation in comparison to PrP-S131C (Figure 3A and B). Interestingly, ΔN showed dimer formation but no neuroprotective activity, suggesting that dimer formation might be necessary but not sufficient for the neuroprotective activity of PrP. Supporting the notion that dimerization of PrP might be linked to its stress-protective activity, dimerization of PrP-S131C was increased after stress treatment (Figure 3C).

To follow up the question whether PrP dimer formation is associated with stress-protective signalling of PrP^C, we used different anti-PrP antibodies to induce PrP dimerization at the plasma membrane. Treatment of cell expressing wt PrP with the antibodies 3F4 and SAF61, which bind adjacent to the HD, induced phosphorylation of ERK, whereas 4H11, which binds directly to the HD, did not (Figure 3D). Moreover, antibody treatment did not induce ERK signalling in cells expressing PrPΔN or PrP-CD4, mutants devoid of a stress-protective activity (Figure 1).

In summary, our data revealed that dimers of PrP^C are present at the plasma membrane of neuronal cells. Dimer formation as well as the stress-protective activity of PrP^C is dependent on the internal HD and the C-terminal GPI anchor.

Scrapie-infected cells are more sensitive to stress and are impaired in PrP^C dimerization

ScN2a cells are chronically scrapie-infected N2a cells that propagate PrP^{Sc} and infectious prions (Butler *et al*, 1988; Caughey and Raymond, 1991; Borchelt *et al*, 1992). In contrast to the uninfected N2a cells, ScN2a cells accumulate significant amounts of detergent-insoluble and protease K-resistant PrP^{Sc} (Figure 4A). When we compared the proliferation rates of ScN2a cells with that of uninfected

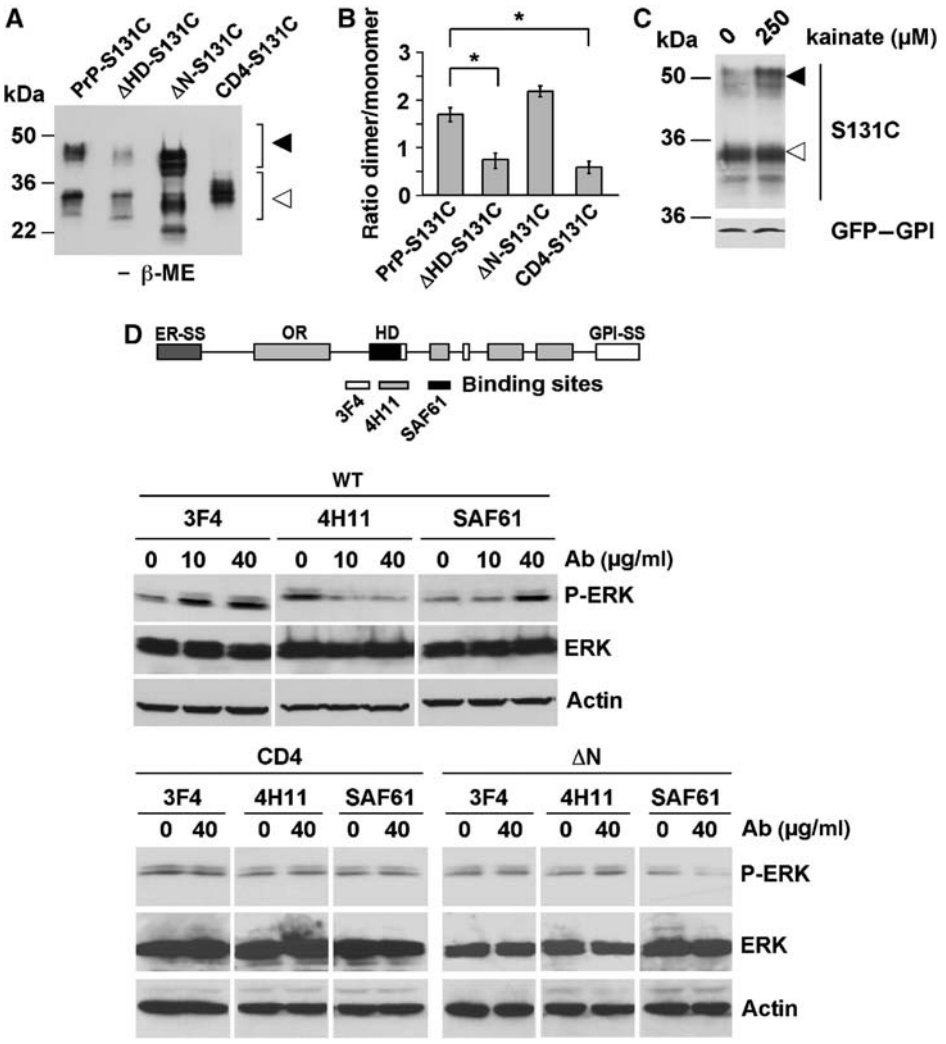

Figure 3 Dimerization of PrP induces intracellular signalling and is dependent on the hydrophobic domain and the GPI anchor. (**A**) Dimerization of PrP is dependent on the hydrophobic domain and the GPI anchor. Wt PrP-S131C, ΔHD-S131C, ΔN-S131C or CD4-S131C was expressed in SH-SY5Y cells and PrP dimers present in total cell lysates were analysed by SDS–PAGE/western blotting under non-reducing conditions. (**B**) Quantification of PrP dimer formation. The ratio of dimeric to monomeric PrP, analysed in at least three independent experiments, is shown. (**C**) Stress-induced dimerization of PrP. SH-SY5Y cells were transfected with S131C or GFP–GPI, incubated with kainate (250 μM) for 2 h at 37°C. PrP and GFP–GPI was detected by western blotting using the mAb 3F4 and the anti-GFP antibody, respectively. (**D**) Antibody-induced signalling of PrP is dependent on the N terminus, the HD and the GPI anchor. SH-SY5Y cells were transfected with wt PrP, PrPΔN or PrPCD4 as indicated. Cells were incubated for 10 min with increasing concentrations of the antibodies 3F4, 4H11 or SAF61, as indicated. P-ERK and ERK were visualized by immunoblotting. Loading was controlled by re-probing the blots for actin. $^*P<0.05$.

N2a cells, it appeared that PrP^{Sc} propagation does not significantly interfere with cell viability (Figure 4B), corroborating earlier results (Bosque and Prusiner, 2000). This picture completely changed, when we analysed cell viability after stress. We subjected N2a and ScN2a cells to heat or oxidative stress and determined cell survival after 24 h. In both stress paradigms, ScN2a cells were significantly more sensitive (Figure 4C and D). In ScN2a cells, the steady-state level of PrP^{C}, present in the detergent-soluble fraction, was at least as high as in N2a cells, suggesting that reduced level of PrP^{C} does not account for the differences in vulnerability to stress (Figure 4A). Next, we analysed PrP-S131C dimer formation in N2a and ScN2a cells at day 2 and 5 after plating. The rationale behind this strategy was the observation that the relative amount of PrP^{Sc} increases over time (Figure 4F). Transfection efficiency was decreased in 5-day-old cells; however, the monomer to dimer ratio was unchanged in N2a cells. In contrast, the relative amount of PrP-S131C dimers negatively correlated with the PrP^{Sc} load: ScN2a cells harbouring less PrP^{Sc} had more dimers compared with cells that had accumulated larger amounts of PrP^{Sc} (Figure 4E and F). To test whether dimeric PrP is a substrate for the formation of PrP^{Sc}, we transfected ScN2a cells and analysed the conversion of the constructs into proteinase K (PK)-resistant PrP. PrPΔHD was not converted, corroborating earlier results (Holscher *et al*, 1998). Interestingly, PrP-S131C was also less efficiently converted into PrP^{Sc}, suggesting that a PrP^{C} dimer is not an optimal substrate for PrP^{Sc} propagation (Figure 4G).

In summary, our experiments revealed that scrapie-infected N2a cells are significantly more vulnerable to stress and that the accumulation of PrP^{Sc} interferes with PrP dimer formation.

Pro-apoptotic signalling of scrapie prions through PrP^{C}

A major question in prion diseases and other neurodegenerative disorders is how misfolded protein conformers induce

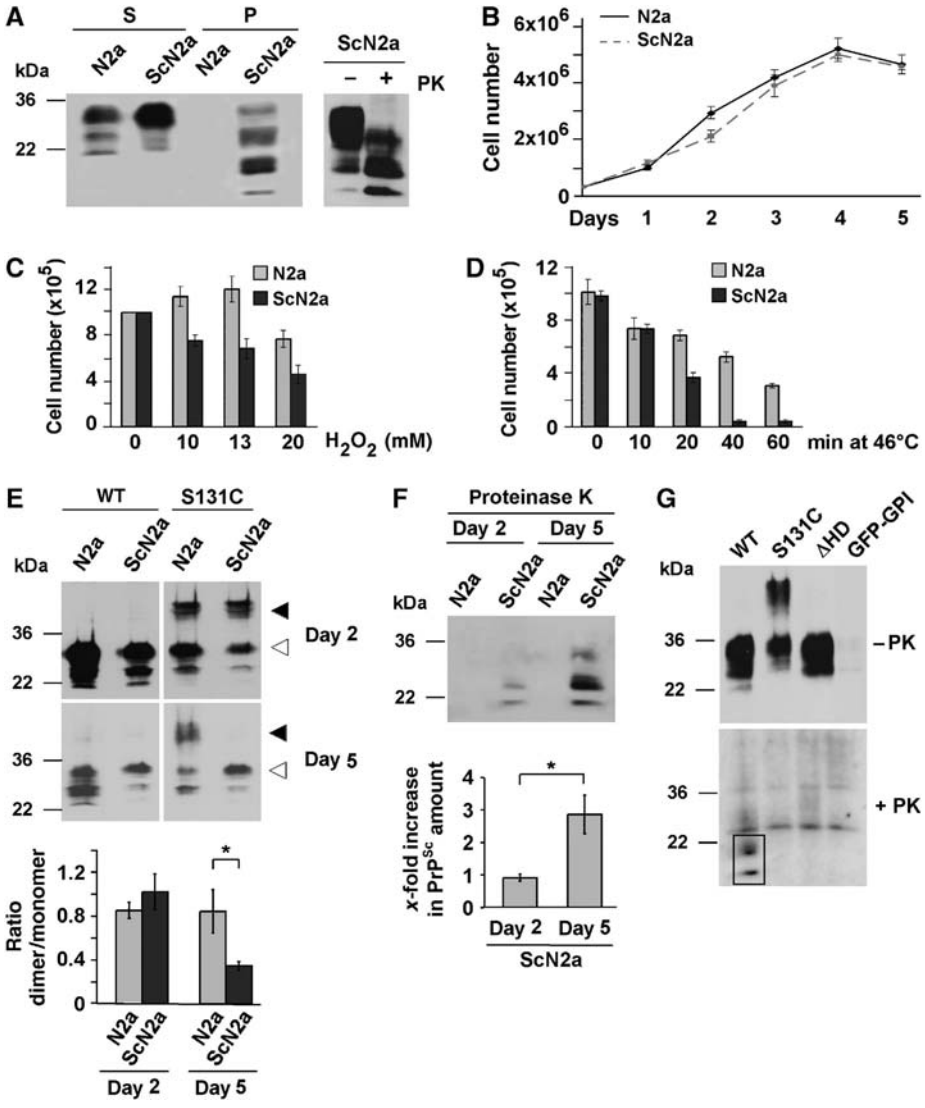

Figure 4 Scrapie prion propagating N2a cells are more susceptible to stress and contain reduced levels of PrP^C dimers. (**A**) ScN2a cells accumulate detergent-insoluble and proteinase K (PK)-resistant PrP. N2a and ScN2a cells were grown for 5 days until confluency. Cells were lysed and PrP present in the detergent-soluble (S) and -insoluble (P) fraction or after a limited PK digest (right panel) was detected by western blotting using the anti-PrP antiserum A7. (**B–D**) Impaired viability of ScN2a cells after stress. (B) Equal number of cells was seeded onto cell culture dishes and cell numbers were determined by counting on 5 consecutive days. (C, D) N2a and ScN2a cells were grown for 4 days and treated with (C) increasing concentrations of H_2O_2 for 30 min or (D) subjected to a heat shock at 46°C for the times indicated. After 24 h cells were counted. Cell death was visualized using Trypan blue. (**E**, **F**) Increased PrP^{Sc} load is paralleled by a decrease in PrP dimerization. N2a and ScN2a cells were transfected with wt PrP or PrP-S131C 1 or 4 days after plating. After additional 24 h (days 2 and 5, respectively) cells were scraped off the plate and lysed. (E) Lysates were analysed *in toto* by SDS–PAGE under non-reducing conditions. PrP was detected using the mAb 3F4. The ratio of dimeric/monomeric PrP was quantified from at least three independent experiments (lower graph). Closed arrowheads indicate dimeric forms of PrP, open arrowheads indicate PrP monomers. (F) Mock-transfected dishes of ScN2a cells (2 and 5 day old) were lysed and treated with PK prior to western blotting. The relative amount of PK-resistant PrP^{Sc} was quantified from at least three independent experiments (lower graph). (**G**) Dimeric PrP cannot be converted to PrP^{Sc}. ScN2a cells were transfected with wt PrP, S131C, PrPΔHD or GFP–GPI and grown for 4 days. Cell lysates were treated with PK and remaining PrP was detected by western blot using the mAb 3F4. PK resistance is highlighted by a black frame. $^*P<0.05$.

neuronal cell death. In prion diseases, neurodegeneration is dependent on the expression of GPI-anchored PrP^C in neuronal cells (Brandner *et al*, 1996; Mallucci *et al*, 2003; Chesebro *et al*, 2005). One possible explanation for this phenomenon is that PrP^C-dependent pathways mediate toxic signalling of PrP^{Sc} or prions. To analyse this possibility in more detail, we developed a novel assay based on the co-cultivation of uninfected cells with persistently infected ScN2a cells. The rationale of this approach was the observation that PrP^{Sc} is actively released into the extracellular environment by PrP-expressing cells (Fevrier *et al*, 2004; Vella *et al*, 2007). SH-SY5Y cells grown on cover slips were transiently transfected with wt PrP, or mutants lacking a stress-protective activity. A cover slip was then placed into a cell culture dish with N2a or ScN2a cells and apoptosis of SH-SY5Y cells was analysed after 16 h in co-culture (Figure 5A). Control-transfected SH-SY5Y cells expressing GPI-anchored GFP could be co-cultivated with N2a or ScN2a cells without adverse effects on cell viability (Figure 5B; GFP–GPI). Similarly, SH-SY5Y cells expressing wt PrP did not undergo apoptosis when co-cultured with uninfected N2a cells. However, a significant increase in apoptotic cell death was observed when SH-SY5Y

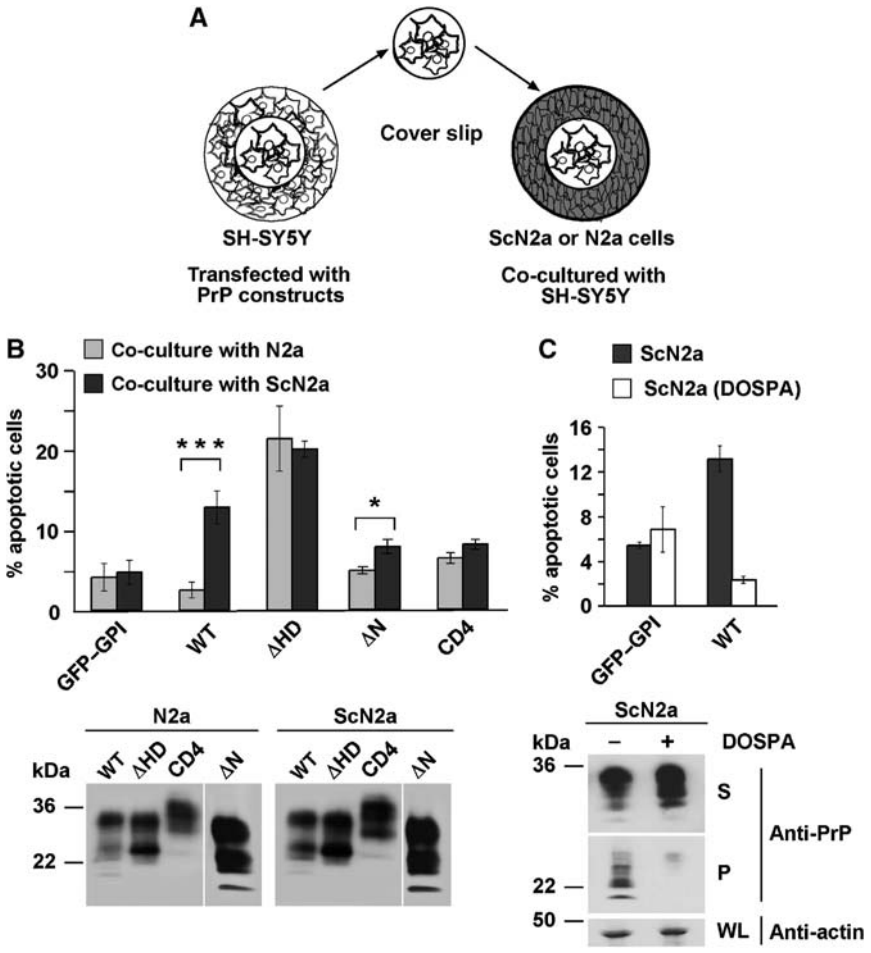

Figure 5 Scrapie prions induce apoptosis in PrP^C-expressing cells. (**A**) Schematic model of the co-cultivation assay. SH-SY5Y cells were grown on cover slips and transfected. At 3 h after transfection, cover slips were transferred to a cell culture dish with N2a or ScN2a cells and co-cultivated for 16 h. (**B**) Scrapie-infected cells induce apoptosis in wt PrP-expressing cells. SH-SY5Y cells were transiently transfected with the constructs indicated and co-cultivated with N2a or ScN2a cells for 16 h. Cells were fixed and stained for activated caspase-3. Apoptotic cells among the transfected were counted in at least three independent experiments. The percentage of apoptotic cells is shown. $***P<0.0005$; $*P<0.05$. Expression of PrP in the SH-SY5Y cells co-cultivated with N2a or ScN2a cells was analysed by immunoblotting using the mAb 3F4. Lower panel: SH-SY5Y cells were transiently transfected with GFP–GPI or wt PrP and co-cultivated with ScN2a or DOSPA-treated ScN2a cells. Apoptotic cell death in the SH-SY5Y cells was determined as described under (B). The western blot image was re-arranged by positioning lane ΔN to the right end of the blot, as indicated by a white line. All samples originate from one gel. (**C**) Parallel dishes of ScN2a and DOSPA-treated ScN2a cells were lysed and PrP present in the detergent-soluble (S) and -insoluble (P) fractions was analysed by western blotting using the anti-PrP antiserum A7 (lower panel). Actin analysed in whole lysates (WL).

cells expressing wt PrP were co-cultivated with ScN2a cells (Figure 5B; wt). As described above, expression of PrPΔHD was toxic to SH-SY5Y cells; however, co-cultivation with ScN2a cells did not increase apoptotic cell death in PrPΔHD-expressing SH-SY5Y cells (Figure 5B; ΔHD). Moreover, PrP-CD4, a mutant defective in stress-protective signalling and dimerization, did not sensitize SH-SY5Y cells to PrP^{Sc}-induced apoptosis (Figure 5B; CD4).

To provide support for the assumption that the inducer of toxicity is PrP^{Sc}, we co-cultivated wt PrP-expressing SH-SY5Y cells with ScN2a cells 'cured' of PrP^{Sc}. We have previously shown that incubation with DOSPA, a cationic lipopolyamine, efficiently reduced the levels of PrP^{Sc} in ScN2a cells (Winklhofer and Tatzelt, 2000). In contrast to untreated ScN2a cells, DOSPA-treated ScN2a cells, which are characterized by a significantly reduced amount of PrP^{Sc}, did not induce apoptosis in PrP-expressing SH-SY5Y cells (Figure 5C).

Thus, our cell culture co-cultivation assay revealed that scrapie-infected cells can induce apoptotic cell death in trans. This toxic signalling was dependent on the propagation of PrP^{Sc} in ScN2a cells and the expression of GPI-anchored wt PrP in co-cultured cells.

Scrapie-induced apoptosis in PrP^C-expressing cells is linked to the activation of the Jun N-terminal kinase and can be blocked by Jun N-terminal kinase inhibitors

The experiments described above provided evidence for an apoptotic process in wt PrP-expressing SH-SY5Y cells when co-cultivated with ScN2a cells. To get insight into the intracellular pathways involved, we analysed key components of apoptotic signalling cascades. We observed phosphorylation of Jun N-terminal kinase (JNK) specifically in wt PrP-expressing SH-SY5Y cells upon co-cultivation with ScN2a cells (Figure 6A, left panel). We did not see consistent activation of ERK or p38 under these conditions, although ERK seems to become slightly activated when co-cultured with ScN2a cells (Figure 6A, middle and right panels). To test whether activation of JNK is linked to the apoptotic cell death of PrP-expressing SH-SY5Y cells, the JNK inhibitor II was added.

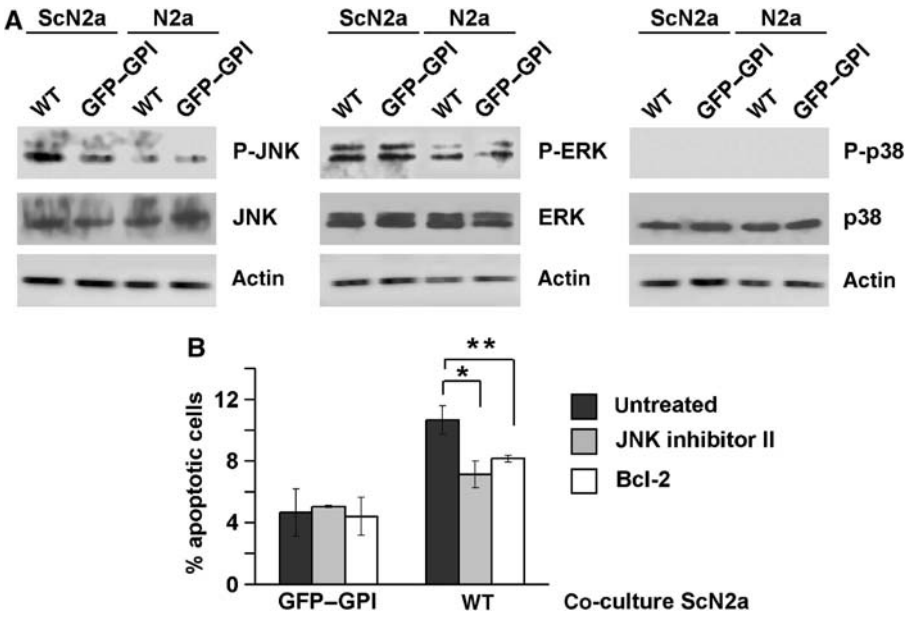

Figure 6 Scrapie prions activate JNK only in wt PrP-expressing cells. (**A**) Co-cultivation with ScN2a cells activates JNK in wt PrP-expressing cells. SH-SY5Y cells were transfected with wt PrP or GFP–GPI and co-cultivated for 16 h with N2a or ScN2a cells. Cells were lysed, and phosphorylated and non-phosphorylated forms of JNK, ERK and p38 were analysed by western blotting. Blots were re-probed for actin to control for equal loading. (**B**) JNK inhibitors interfere with scrapie prion-induced apoptosis. Cells were transfected with GFP–GPI or wt PrP and incubated with the JNK inhibitor II (for 16 h, 1 μM) or co-transfected with Bcl-2. Cells were co-cultivated for 16 h with ScN2a cells, fixed and stained for activated caspase-3. Apoptotic cells were counted and the percentage of apoptotic to transfected cells was evaluated, $*P<0.05$, $**P<0.005$.

Indeed, cell death in PrP-expressing SH-SY5Y co-cultured with ScN2a cells was significantly reduced in the presence of the JNK inhibitor (Figure 6B). A similar reduction in apoptotic cell death was achieved by co-expressing the anti-apoptotic protein Bcl-2. The functionality of the JNK inhibitor was verified in cells exposed to anisomycin (data not shown).

Discussion

Stress-protective signalling of PrP: a prominent role for the internal HD

In our study, we analysed various PrP mutants to define determinants of the neuroprotective activity of PrP^C. First, we showed that expression of wt PrP conferred enhanced stress tolerance to cells, whereas deletion of the unstructured N terminus abolished this activity, corroborating previous findings in mice. Next, we identified two novel domains linked to the stress-protective activity of PrP: the internal HD and the C-terminal GPI anchor. PrP-CD4, a mutant with a transmembrane domain instead of a GPI anchor, is complex glycosylated and present at the outer leaflet of the plasma membrane; however, PrPCD4 is not targeted to detergent-insoluble microdomains. Possibly, PrP-CD4 cannot interact with a, yet unidentified, transmembrane protein necessary to induce signal transduction. The GPI anchor might provide a higher degree of structural flexibility favouring intermolecular interactions at the plasma membrane, or targeting of PrP to detergent-insoluble microdomains is a prerequisite for such an interaction.

Our study reinforces the prominent role of the internal HD in stress-protective signalling of PrP. Expression of PrPΔHD can lead to apoptotic cell death and co-expression of wt PrP^C interferes with pro-apoptotic signalling of PrPΔHD. Our functional characterization of the HD allows the conclusion that the stress-protective signalling of wt PrP^C is linked to dimer formation with the HD as part of the dimer interface. The analysis of PrP^C in cultured cells and mouse brain by native PAGE and crosslinking approaches provided experimental evidence that wt PrP can form homo-dimers and that deletion of the HD interferes with dimer formation. Further evidence was obtained by introducing a cysteine into the HD (PrP-S131C). Such an approach was successfully used to identify the dimerization domain of the transmembrane receptor ErbB-2/Her2 (Cao *et al*, 1992) and the amyloid precursor protein (Munter *et al*, 2007). Similarly to wt PrP, the PrP-S131C dimer was complex glycosylated, present at the plasma membrane in detergent-insoluble microdomains (rafts) and could be liberated by PIPLC digestion. Previous *in vitro* studies indicated that native PrP^C purified from bovine brain exists as a monomer–dimer equilibrium, but not recombinant PrP, suggesting that post-translational modifications might be implicated in dimer formation (Meyer *et al*, 2000). This is in line with our observation that the GPI anchor is necessary for dimer formation. The formation of PrP dimers upon overexpression of hamster PrP in mouse cells was previously described (Priola *et al*, 1995), which seem to be different from the PrP dimers we describe in our study. Notably, the dimers we describe rapidly dissociate in the presence of SDS, are formed in a post-Golgi compartment and are complex glycosylated (Supplementary Figure 1).

On the basis of our data presented above and available NMR analysis (Riek *et al*, 1998; Liu *et al*, 1999), we built models of a PrP^C dimer present at the cell surface (Figure 7). The dimer models were created by docking two identical PrP monomers with cysteines introduced at position 131, and looking for docking configurations, where the two opposing cysteines were positioned at a disulphide bridge distance. Figure 7 depicts two configurations, one, where both

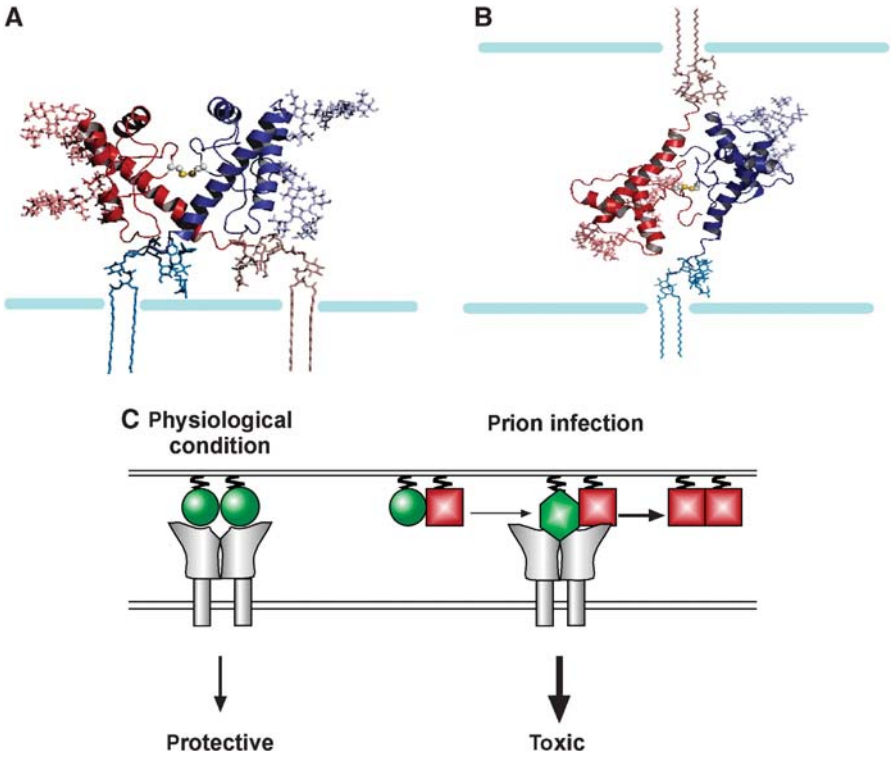

Figure 7 Putative model structures of a PrP^C dimmer. (**A**) Both monomers attached to the same cell. (**B**) 'Trans' dimer: monomers attached to neighbouring cells. The PrP dimers appear in cartoon representation, with the side chains of the cysteine residues in sphere representation; the Asn181 and Asn197-linked N-glycans and the GPI anchors appear in stick representations, whereas the membrane is a schematic drawing. Colouring scheme: the two monomers are in red and blue; the glycans and GPI anchor attached to the red monomer are coloured in red shades, and the ones attached to the blue monomer appear in blue shades, respectively. (**C**) A model for the stress-protective signalling of PrP^C under physiological conditions and pro-apoptotic signalling induced by PrP^{Sc}. PrP^C: green circle; PrP^{Sc}: red square; toxic conformer: green diamond; putative PrP receptor: grey. The model suggests the following scenario: (1) PrP^C dimerizes and can induce protective signalling through a putative transmembrane receptor (either in trans or in cis). (2) Interaction of PrP^C with PrP^{Sc} is leading to a pathogenic PrP complex, which is still able to interact with the putative PrP^C receptor; however, the interaction leads to an aberrant, toxic signalling.

monomers were attached to the same cell (Figure 7A), and the other configuration where the monomers were attached to adjacent cells (Figure 7B).

Different lines of evidence support the scenario that dimer formation of PrP^C is essential for its neuroprotective activity. First, two PrP mutants impaired in dimer formation, PrPΔHD and PrP-CD4, did not protect cells from stress-induced cell death. Second, stress treatment induced PrP dimerization. Third, scrapie prions interfere with dimer formation and the stress-protective activity of PrP^C. However, dimer formation of PrP^C seems to be required but not sufficient for its stress-protective activity: a PrP mutant lacking the unstructured N-terminal domain does not confer enhanced stress tolerance to cells. Cellular targeting and dimerization of PrPΔN is not impaired, but the N-terminal domain might be required for a productive interaction of PrP with its putative co-receptor or for endocytosis of the signalling complex.

Toxic signalling of scrapie prions in PrP^C-expressing cells

Grafting experiments provided the first evidence that PrP^{Sc} is not toxic to neurons devoid of PrP^C (Brandner *et al*, 1996), which was corroborated by additional studies (Mallucci *et al*, 2003; Chesebro *et al*, 2005). On the basis of these animal models, two plausible scenarios for the toxic effects of PrP^{Sc} can be envisaged. Either, neurotoxicity of PrP^{Sc} is linked to its propagation in neuronal cells, which is dependent on the expression of PrP^C, or PrP^{Sc} elicits a deadly signal through a PrP^C-dependent signalling pathway. Please note that we are using PrP^{Sc} as provisional term for a pathological conformer of PrP with neurotoxic activity. Whether this is a PK-resistant intermediate generated during the conversion process or an oligomer or fibril is unclear at the moment. Similarly, it might well be that the neurotoxic and the infectious PrP conformers are distinct species. Indeed, the existence of discrete conformers would explain the phenomenon of subclinical prion infection (Hill *et al*, 2000).

We developed a new co-cultivation assay based on the fact that PrP^{Sc} is actively released into the extracellular environment through exosomes from scrapie-infected cells (Fevrier *et al*, 2004; Vella *et al*, 2007). This allowed us to study the toxic effects of prion replication mechanistically. Co-cultivation with ScN2a cells induced apoptosis in SH-SY5Y cells, but only when the latter transiently expressed wt PrP. N2a or ScN2a cells cured of PrP^{Sc} did not induce apoptosis, indicating that the apoptotic effect was dependent on the presence of PrP^{Sc}. Scrapie prion-induced cell death was paralleled by the activation of JNK in SH-SY5Y cells, and the addition of a JNK inhibitor to the co-cultivation medium significantly reduced apoptotic cell death in SH-SY5Y cells, providing a causal link between JNK activation and PrP^{Sc}-induced apoptosis. This is in line with the observation that JNK is activated in the brains of scrapie-infected mice and hamsters (Carimalo *et al*, 2005; Lee *et al*, 2005).

Table I Characteristic features of the PrP constructs used in this study

PrP	Cell surface	DRM	Stress protective	Toxic	PrP^{Sc} mediated	Conversion into PrP^{Sc}
WT	+	+	+	–	+ +	+ +
S131C	+	+	+	–	+[a]	–
ΔN	+	+	–	–	+	+[b]
ΔHD	+	+	–	+	–	–
CD4	+	–	–	–	–	–[b]

DRM: detergent-resistant membranes.
[a]Data not shown.
[b]From previous publications.

Remarkably, our co-cultivation approach revealed that neurotoxic signalling induced by scrapie prions was dependent on a physiologically active PrP^{C} (Table I). Expression of PrP mutants impaired in their stress-protective potential, such as PrPΔN or PrP-CD4, did not sensitize SH-SY5Y cells to PrP^{Sc}-induced toxicity. In line with this observation, PrPΔHD expression was toxic *per se*; however, PrP^{Sc} did not increase the toxicity of PrPΔHD. How can our data be brought together to explain the PrP^{C}-dependent effects of PrP^{Sc}? PrP^{Sc} could modulate the interaction of PrP^{C} with its putative co-receptor, possibly due to the formation of a PrP^{C}/PrP^{Sc} complex. As a consequence, there is a switch from a stress-protective to a pro-apoptotic signalling, possibly due to over-stimulation of the receptor (Figure 7C). Indeed, pro-apoptotic signalling by PrP^{C} can be induced *in vivo* by antibody-induced crosslinking (Solforosi *et al*, 2004). Compatible with the model of a common receptor for both apoptotic and antiapoptotic signalling is the toxic potential of PrPΔHD. As suggested previously (Baumann *et al*, 2007; Li *et al*, 2007), deletion of the HD might alter the conformation of PrP and thereby the interaction with the PrP^{C} co-receptor, resulting in toxic signalling.

We have now to await the identification of the signalling complex(es) to provide further experimental evidence for such pathways. A better understanding of the auxiliary components implicated in the physiological activity of PrP^{C} and neurotoxic signalling of pathogenic PrP mutants will not only enhance our understanding of stress-induced signalling cascades in neuronal cells but might also allow to develop novel strategies for the treatment of prion diseases.

Materials and methods

Antibodies and reagents

The following antibodies were used: anti-PrP 3F4 monoclonal antibody (mAb; Kascsak *et al*, 1987), anti-PrP antiserum A7 (Winklhofer *et al*, 2003a), anti-active caspase-3 polyclonal antibody (Promega), anti-FLAG M2 mouse mAb (Sigma), Cy3-conjugated anti-rabbit IgG antibody (Dianova), anti-phospho-SAPK/JNK, anti-phospho-p38, anti-phospho-p42/44, anti-JNK, anti-p38 and anti-ERK (Cell Signaling). The following reagents were used: kainic acid (Calbiochem), JNK inhibitor II (Calbiochem), endoglycosidase H (endoH; Calbiochem), peptide *N*-glycosidase F (PNGaseF; Calbiochem), proteinase-K (PK; Sigma), Brefeldin A (Sigma), 3,3′-dithiobis[sulphosuccinimidylpropionate] (DTSSP; Pierce). The mounting medium Mowiol (Calbiochem) was supplemented with 4′,6-diamidino-2-phenylindole (DAPI; Sigma).

Plasmids

The following constructs were described previously: wt PrP, PrP-CD4, T183A (Winklhofer *et al*, 2003b; Kiachopoulos *et al*, 2005) and FLAG–Bcl-2 (Rambold *et al*, 2006). All amino-acid numbers refer to the mouse PrP sequence (GenBank™ accession number NP 035300) or to human Bcl-2 sequence (GenBank™ accession number AAA51813). In PrPΔHD, the amino acids 113–133 were deleted. For the generation of PrP-S131C a serine at position 131 was exchanged to a cysteine. In PrPΔHD-S131C, the amino acids 112–128 were deleted. As transfection marker the EYFP-C1 vector (Clontech) was used.

Cell culture, co-cultivation and curing experiments

Cells were cultivated and transfected as described earlier (Winklhofer and Tatzelt, 2000; Winklhofer *et al*, 2003b). For co-cultivation experiments, SH-SY5Y cells were grown on glass cover slips and transfected with LipofectAMINE Plus reagent. At 3 h after transfection, cover slips were transferred into dishes containing a 90% confluent cell layer of either N2a or ScN2a cells. After 16 h in co-culture, apoptotic cell death in SH-SY5Y cells was analysed (see below). ScN2a cells were cured of PrP^{Sc} by treatment with DOSPA (Winklhofer and Tatzelt, 2000).

Cell lysis, detergent solubility assay, western blotting and sucrose step gradient

As described earlier (Tatzelt *et al*, 1996), cells were washed twice with cold PBS, scraped off the plate and lysed in cold buffer A (0.5% Triton X-100, 0.5% sodium deoxycholate in PBS). The lysates were either analysed directly or centrifuged to generate detergent-soluble (S) and -insoluble (P) fractions. SDS–PAGE and western blotting was described earlier (Winklhofer and Tatzelt, 2000). For the detection of phosphorylated proteins, cells were lysed in cold buffer B (20 mM Tris (pH 7.5), 150 mM NaCl, 1 mM EDTA, 1 mM EGTA, 1% Triton X-100, 2.5 mM sodium pyrophosphate, 1 mM b-glycerophosphate, 1 mM Na_3Vo_4 and 1 μg/ml leupeptin), centrifuged for 10 min at 13 000 r.p.m. and the postnuclear supernatant was analysed by western blotting according to the manufacturer's instruction. For the sucrose step, gradient cells were harvested and resuspended in 200 μl buffer C (25 mM MES, 150 mM NaCl, pH 6.5) containing 1% Triton X-100 and homogenized by passing 15 times through a Luer 21-gauge needle. After centrifugation at 500 *g* for 5 min, the supernatant was made up to 40% sucrose by adding an equal volume of 80% sucrose in buffer C. The sample was placed beneath a discontinuous gradient of sucrose consisting of 3 ml of 30% sucrose and 1 ml of 5% sucrose, both in buffer C. The samples were then centrifuged at 140 000 *g* in a SW-55 rotor (Beckman Coulter) for 18 h at 4°C. The sucrose gradient was harvested in 0.5 ml fractions from the top of the gradient, precipitated by TCA and analysed by western blotting.

Chemical crosslinking

Transfected N2a, SH-SY5Y cells or total mouse brain were lysed by addition of 150 μl or 1 ml of crosslinking buffer (250 mM sucrose, 5 mM Hepes (pH 7,4), 1 mM $MgCl_2$ and 10 mM KCl), respectively, and passing 15 times through a Luer 21-gauge needle. After centrifugation for 20 min at 800 *g*, the supernatant was incubated with the chemical crosslinker DTSSP for 1 h at 4°C as specified by the manufacturer, at the concentrations indicated. Proteins were precipitated by TCA and analysed by western blotting.

Conversion assay

ScN2a cells were transfected with 2 μg DNA and grown for 4 days until total confluency. Cells were lysed in cold buffer A and centrifuged for 1 min at 1000 *g*. The supernatant was incubated with 10 μg/ml PK for 40 min at 22°C and the reaction was quenched by

addition of 2 mM PMSF. Residual proteins were precipitated by TCA and transfected PrP was detected by western blotting using the mAb 3F4.

Stress induction, phospholipase C and JNK inhibitor treatment

Kainic acid was dissolved in water and added to the cell culture medium. JNK inhibitor II was dissolved in water and cells were incubated with 1 μM for 16 h at 37°C during co-cultivation. Phospholipase C treatment was described earlier (Winklhofer *et al*, 2003b). Briefly, cells were washed twice with ice-cold PBS and PIPLC in PBS was added to the cells for 3 h at 37°C. Cell culture supernatants were collected and proteins were precipitated by TCA.

Native PAGE

PrP-transfected SH-SY5Y cells were treated with PIPLC and proteins in the cell culture supernatant were collected and concentrated by centrifugation at 1000 *g* for 15 min at 4°C in Vivaspin tubes (excision size: 30 000 MW; Vivascience). Sample buffer (6 ×; 360 mM Tris–HCl (pH 6.8), 60% glycerol, 0.4% Coomassie blue brilliant servablue) was added to the concentrated samples and the samples were loaded on native gels. Native gels consisted of stacking gel (4% acrylamid, 150 mM Tris–HCl (pH 6.8), 0.1% TEMED, 0.1% APS) and resolving gel (8% acrylamid, 375 mM Tris–HCl (pH 8.8), 0.1% TEMED, 0.1% APS). Gel running was performed in gel running buffer (25 mM Tris and 189 mM glycine) for 4 h with increasing working voltage (80–180 V). The proteins were transferred to a PVDF membrane (Millipore Immobilon) in blotting buffer (20 mM Tris, 150 mM glycine and 20% methanol) for 60 min at 80 V. The membrane was dried and extensively washed in isopropanol, neutralized in H_2O for 1 min, washed with PBST for 10 min and blocked with 5% milk in PBST.

Proliferation and cell survival measurements

Equal cell numbers of N2a and ScN2a cells were seeded. The proliferation rate of both cell lines was determined by counting trypsinated cells daily over a period of 5 days using a Neubauer-counting chamber. For cell survival measurements, cells were stressed 4 days after seeding with H_2O_2 for 30 min, or subjected to a 46°C heat shock. At 24 h after stress treatment, cells were trypsinated and the number of live cells was determined by Trypan blue exclusion assay.

Apoptosis assay

As described before (Rambold *et al*, 2006), SH-SY5Y cells were grown on glass cover slips, fixed with 3% PFA for 20 min and permeabilized with 0.2% Triton X-100 in PBS for 10 min at room temperature. The primary antibody anti-active caspase-3 was incubated for 45 min at 37°C in 1% BSA. After extensive washing with cold PBS, incubation with the Cy3-conjugated secondary antibody followed at 20°C for 90 min. Cells were mounted onto glass slides and examined by fluorescence microscopy using a Zeiss Axiovert 200 M microscope (Carl Zeiss). The number of activated caspase-3-positive cells out of 300 transfected cells was determined. All quantifications were based on triplicates of at least three independent experiments.

Generation of the PrP dimer model

The PrP dimer was built by docking two copies of the known structure of a PrP monomer to each other. The monomer structure used was the NMR structure of the mouse prion protein domain mPrP (amino acids 121–231) solved by Wutrich's group (pdb file: 1XYX) (Riek *et al*, 1998). A cysteine residue was introduced by inserting a S131C substitution using the NEST homology modeling package (Petrey *et al*, 2003), with default parameters. To create the S-S-bonded dimer, two identical monomers were docked, using the ZDOCK software (http://zlab.bu.edu/zdock) (Mintseris *et al*, 2005); ZDOCK is a rigid-body docking software that searches for possible binding configurations of the proteins, and evaluates them based on shape complementarity, desolvation energy and electrostatics. ZDOCK provides a series of putative docking configurations. Docking was limited to configurations in which the contact between the monomers involved the cysteines and their surroundings. The resulting predicted structures were then filtered for configurations in which the cysteines were at a distance of 6 Å or less. Thereafter, the cysteines were bonded using the PyMol.

Statistical analysis

Data were expressed as means ± s.e. All experiments were performed in triplicates and repeated at least three times. Statistical analysis among groups was performed using student's *t*-test. *P*-values are as follows: $^{*}P<0.05$, $^{**}P<0.005$ and $^{***}P<0.0005$.

Supplementary data

Supplementary data are available at *The EMBO Journal* Online (http://www.embojournal.org).

Acknowledgements

We are grateful to Christian Haass for continuous support and stimulating discussions. We thank Margit Miesbauer for critically reading the paper and for helpful discussions. This study was supported by grants from the Deutsche Forschungsgemeinschaft (SFB 596), the Max Planck Society and the BMBF (BioDisc, DIP5.1).

References

Aguzzi A, Polymenidou M (2004) Mammalian prion biology: one century of evolving concepts. *Cell* **116:** 313–327

Baumann F, Tolnay M, Brabeck C, Pahnke J, Kloz U, Niemann HH, Heikenwalder M, Rulicke T, Burkle A, Aguzzi A (2007) Lethal recessive myelin toxicity of prion protein lacking its central domain. *EMBO J* **26:** 538–547

Borchelt DR, Taraboulos A, Prusiner SB (1992) Evidence for synthesis of scrapie prion proteins in the endocytic pathway. *J Biol Chem* **267:** 16188–16199

Bosque PJ, Prusiner SB (2000) Cultured cell sublines highly susceptible to prion infection. *J Virol* **74:** 4377–4386

Brandner S, Isenmann S, Raeber A, Fischer M, Sailer A, Kobayashi Y, Marino S, Weissmann C, Aguzzi A (1996) Normal host prion protein necessary for scrapie-induced neurotoxicity. *Nature* **379:** 339–343

Büeler H, Aguzzi A, Sailer A, Greiner R-A, Autenried P, Aguet M, Weissmann C (1993) Mice devoid of PrP are resistant to scrapie. *Cell* **73:** 1339–1347

Butler DA, Scott MRD, Bockman JM, Borchelt DR, Taraboulos A, Hsiao KK, Kingsbury DT, Prusiner SB (1988) Scrapie-infected murine neuroblastoma cells produce protease-resistant prion proteins. *J Virol* **62:** 1558–1564

Cao H, Bangalore L, Dompe C, Bormann BJ, Stern DF (1992) An extra cysteine proximal to the transmembrane domain induces differential cross-linking of p185neu and p185neu. *J Biol Chem* **267:** 20489–20492

Carimalo J, Cronier S, Petit G, Peyrin JM, Boukhtouche F, Arbez N, Lemaigre-Dubreuil Y, Brugg B, Miquel MC (2005) Activation of the JNK-c-Jun pathway during the early phase of neuronal apoptosis induced by PrP106-126 and prion infection. *Eur J Neurosci* **21:** 2311–2319

Caughey B, Raymond GJ (1991) The scrapie-associated form of PrP is made from a cell surface precursor that is both protease- and phospholipase-sensitive. *J Biol Chem* **266:** 18217–18223

Chesebro B (2003) Introduction to the transmissible spongiform encephalopathies or prion diseases. *Br Med Bull* **66:** 1–20

Chesebro B, Trifilo M, Race R, Meade-White K, Teng C, LaCasse R, Raymond L, Favara C, Baron G, Priola S, Caughey B, Masliah E, Oldstone M (2005) Anchorless prion protein results in infectious amyloid disease without clinical scrapie. *Science* **308:** 1435–1439

Collinge J (2001) Prion diseases of humans and animals: their causes and molecular basis. *Annu Rev Neurosci* **24:** 519–550

Fevrier B, Vilette D, Archer F, Loew D, Faigle W, Vidal M, Laude H, Raposo G (2004) Cells release prions in association with exosomes. *Proc Natl Acad Sci USA* **101:** 9683–9688

Hill AF, Joiner S, Linehan J, Desbruslais M, Lantos PL, Collinge J (2000) Species-barrier-independent prion replication in apparently resistant species. *Proc Natl Acad Sci USA* **97:** 10248–10253

Holscher C, Delius H, Burkle A (1998) Overexpression of nonconvertible PrPc delta114–121 in scrapie-infected mouse neuroblastoma cells leads to trans-dominant inhibition of wild-type PrP(Sc) accumulation. *J Virol* **72:** 1153–1159

Kascsak RJ, Rubenstein R, Merz PA, Tonna-DeMasi M, Fersko R, Carp RI, Wisniewski HM, Diringer H (1987) Mouse polyclonal and monoclonal antibody to scrapie-associated fibril proteins. *J Virol* **61:** 3688–3693

Kiachopoulos S, Bracher A, Winklhofer KF, Tatzelt J (2005) Pathogenic mutations located in the hydrophobic core of the prion protein interfere with folding and attachment of the glycosylphosphatidylinositol anchor. *J Biol Chem* **280:** 9320–9329

Kuwahara C, Takeuchi AM, Nishimura T, Haraguchi K, Kubosaki A, Matsumoto Y, Saeki K, Matsumoto Y, Yokoyama T, Itohara S, Onodera T (1999) Prions prevent neuronal cell-line death. *Nature* **400:** 225–226

Lee HP, Jun YC, Choi JK, Kim JI, Carp RI, Kim YS (2005) Activation of mitogen-activated protein kinases in hamster brains infected with 263K scrapie agent. *J Neurochem* **95:** 584–593

Li A, Christensen HM, Stewart LR, Roth KA, Chiesa R, Harris DA (2007) Neonatal lethality in transgenic mice expressing prion protein with a deletion of residues 105–125. *EMBO J* **26:** 548–558

Liu H, Farr-Jones S, Ulyanov NB, Llinas M, Marqusee S, Groth D, Cohen FE, Prusiner SB, James TL (1999) Solution structure of Syrian hamster prion protein rPrP(90–231). *Biochemistry* **38:** 5362–5377

Mallucci G, Dickinson A, Linehan J, Klohn PC, Brandner S, Collinge J (2003) Depleting neuronal PrP in prion infection prevents disease and reverses spongiosis. *Science* **302:** 871–874

McLennan NF, Brennan PM, McNeill A, Davies I, Fotheringham A, Rennison KA, Ritchie D, Brannan F, Head MW, Ironside JW, Williams A, Bell JE (2004) Prion protein accumulation and neuroprotection in hypoxic brain damage. *Am J Pathol* **165:** 227–235

Meyer RK, Lustig A, Oesch B, Fatzer R, Zurbriggen A, Vandevelde M (2000) A monomer–dimer equilibrium of a cellular prion protein (PrPC) not observed with recombinant PrP. *J Biol Chem* **275:** 38081–38087

Mintseris J, Wiehe K, Pierce B, Anderson R, Chen R, Janin J, Weng Z (2005) Protein–protein docking benchmark 2.0: an update. *Proteins* **60:** 214–216

Mitteregger G, Vosko M, Krebs B, Xiang W, Kohlmannsperger V, Nolting S, Hamann GF, Kretzschmar HA (2007) The role of the octarepeat region in neuroprotective function of the cellular prion protein. *Brain Pathol* **17:** 174–183

Munter LM, Voigt P, Harmeier A, Kaden D, Gottschalk KE, Weise C, Pipkorn R, Schaefer M, Langosch D, Multhaup G (2007) GxxxG motifs within the amyloid precursor protein transmembrane sequence are critical for the etiology of Abeta42. *EMBO J* **26:** 1702–1712

Petrey D, Xiang Z, Tang CL, Xie L, Gimpelev M, Mitros T, Soto CS, Goldsmith-Fischman S, Kernytsky A, Schlessinger A, Koh IY, Alexov E, Honig B (2003) Using multiple structure alignments, fast model building, and energetic analysis in fold recognition and homology modeling. *Proteins* **53** (Suppl 6)**:** 430–435

Priola SA, Caughey B, Wehrly K, Chesebro B (1995) A 60-kDa prion protein (PrP) with properties of both the normal and scrapie-associated forms of PrP. *J Biol Chem* **270:** 3299–3305

Prusiner SB, Scott MR, DeArmond SJ, Cohen FE (1998) Prion protein biology. *Cell* **93:** 337–348

Rambold AS, Miesbauer M, Rapaport D, Bartke T, Baier M, Winklhofer KF, Tatzelt J (2006) Association of Bcl-2 with misfolded prion protein is linked to the toxic potential of cytosolic PrP. *Mol Biol Cell* **17:** 3356–3368

Riek R, Wider G, Billeter M, Hornemann S, Glockshuber R, Wuthrich K (1998) Prion protein NMR structure and familial human spongiform encephalopathies. *Proc Natl Acad Sci USA* **95:** 11667–11672

Shmerling D, Hegyi I, Fischer M, Blättler T, Brandner S, Götz J, Rülicke T, Flechsig E, Cozzio A, von Mehring C, Hangartner C, Aguzzi A, Weissmann C (1998) Expression of amino-terminally truncated PrP in the mouse leading to ataxia and specific cerebellar lesions. *Cell* **93:** 203–214

Shyu WC, Lin SZ, Chiang MF, Ding DC, Li KW, Chen SF, Yang HI, Li H (2005) Overexpression of PrPC by adenovirus-mediated gene targeting reduces ischemic injury in a stroke rat model. *J Neurosci* **25:** 8967–8977

Solforosi L, Criado JR, McGavern DB, Wirz S, Sanchez-Alavez M, Sugama S, DeGiorgio LA, Volpe BT, Wiseman E, Abalos G, Masliah E, Gilden D, Oldstone MB, Conti B, Williamson RA (2004) Cross-linking cellular prion protein triggers neuronal apoptosis *in vivo*. *Science* **303:** 1514–1516

Spudich A, Frigg R, Kilic E, Kilic U, Oesch B, Raeber A, Bassetti CL, Hermann DM (2005) Aggravation of ischemic brain injury by prion protein deficiency: role of ERK-1/-2 and STAT-1. *Neurobiol Dis* **20:** 442–449

Taraboulos A, Scott M, Semenov A, Avrahami D, Laszlo L, Prusiner SB (1995) Cholesterol depletion and modification of COOH-terminal targeting sequence of the prion protein inhibit formation of the scrapie isoform. *J Cell Biol* **129:** 121–132

Tatzelt J, Prusiner SB, Welch WJ (1996) Chemical chaperones interfere with the formation of scrapie prion protein. *EMBO J* **15:** 6363–6373

Vella LJ, Sharples RA, Lawson VA, Masters CL, Cappai R, Hill AF (2007) Packaging of prions into exosomes is associated with a novel pathway of PrP processing. *J Pathol* **211:** 582–590

Warwicker J (2000) Modeling a prion protein dimer: predictions for fibril formation. *Biochem Biophys Res Commun* **278:** 646–652

Weise J, Sandau R, Schwarting S, Crome O, Wrede A, Schulz-Schaeffer W, Zerr I, Bahr M (2006) Deletion of cellular prion protein results in reduced Akt activation, enhanced postischemic caspase-3 activation, and exacerbation of ischemic brain injury. *Stroke* **37:** 1296–1300

Weissmann C, Fischer M, Raeber A, Büeler H, Sailer A, Shmerling D, Rülicke T, Brandner S, Aguzzi A (1996) The role of PrP in pathogenesis of experimental scrapie. *Cold Spring Harb Symp Quant Biol* **61:** 511–522

Westergard L, Christensen HM, Harris DA (2007) The cellular prion protein (PrP(C)): its physiological function and role in disease. *Biochim Biophys Acta* **1772:** 629–644

Winklhofer KF, Heller U, Reintjes A, Tatzelt J (2003a) Inhibition of complex glycosylation increases formation of PrPSc. *Traffic* **4:** 313–322

Winklhofer KF, Heske J, Heller U, Reintjes A, Muranji W, Moarefi I, Tatzelt J (2003b) Determinants of the *in vivo*-folding of the prion protein: a bipartite function of helix 1 in folding and aggregation. *J Biol Chem* **278:** 14961–14970

Winklhofer KF, Tatzelt J (2000) Cationic lipopolyamines induce degradation of PrPSc in scrapie-infected mouse neuroblastoma cells. *Biol Chem* **381:** 463–469

Winklhofer KF, Tatzelt J, Haass C (2008) The two faces of protein misfolding: gain and loss of function in neurodegenerative diseases. *EMBO J* **27:** 336–349

